Imaging of calcium transients in skeletal muscle fibers

Julio Vergara,* Marino DiFranco,‡ Deida Compagnon,* and Benjamin A. Suarez-Isla§
*Department of Physiology, University of California Los Angeles, Los Angeles, California 90024 USA; ‡Laboratorio de Fisiologia Animal, Escuela de Biologia, Universidad Central de Venezuela, Caracas, Venezuela; and §Centro de Estudios Cientificos de Santiago and Departamento de Fisiologia y Biofisica, Facultad de Medicina, Universidad de Chile, Santiago, Chile

ABSTRACT Epifluorescence images of Ca^{2+} transients elicited by electrical stimulation of single skeletal muscle fibers were studied with fast imaging techniques that take advantage of the large fluorescence signals emitted at relatively long wavelengths by the dyes fluo-3 and rhod-2 in response to binding of Ca^{2+} ions, and of the suitable features of a commercially available CCD video camera. The localized release of Ca^{2+} in response to microinjection of $InsP_3$ was also monitored to demonstrate the adequate space and time resolutions of the imaging system. The time resolution of the imager system, although limited to the standard video frequency response, still proved to be adequate to investigate the fast Ca^{2+} release process in skeletal muscle fibers at low temperatures.

INTRODUCTION

It is well known that the Ca^{2+} transients elicited by electrical stimulation of single skeletal muscle fibers reach peak values shortly after the onset of the stimulus, between a few milliseconds to tens of milliseconds depending on the temperature of the experiment (Miledi et al., 1977; Vergara and Delay, 1986). The fast time course of this transient has been previously monitored with the photoprotein aequorin (Blinks et al., 1978), metallochromic indicators (Baylor et al., 1982; Miledi et al., 1982; Palade and Vergara, 1982; Kovacz et al., 1983; Vergara and Delay, 1986; Hirota et al., 1989), and fura-2 (Baylor and Hollingworth, 1988) using detector devices, such as photodiodes or photomultipliers, which respond to changes in light intensity with minimal delays at a bandwidth ranging from DC up to 5 KHz.

Calcium imaging techniques, based mostly in the use of the fluorescent indicators fura-2 and indo-1, have been utilized in a number of biological preparations to investigate cell calcium metabolism (Williams et al., 1985; Wier et al., 1987; Lipscombe et al., 1988*a*, *b*; Kawanishi et al., 1989; see also a review by Tsien, 1988). These techniques permit continuous monitoring of the intracellular calcium concentration ($[Ca^{2+}]_i$), providing valuable information about the distribution of this ion in different subregions of the cell. Cellular processes, like the diffusion of Ca^{2+} in the cytosol (Lipscombe et al., 1988*a*), the generation of $[Ca^{2+}]_i$ oscillations (Cannel et al., 1987; Lipscombe et al., 1988*a*, *b*; Kawanishi et al., 1989), the intercellular communication and propagation of Ca^{2+} waves (Cornell-Bell et al., 1990), and the release of Ca^{2+} from intracellular stores (Wier et al., 1987; Cannel et al., 1987; Lipscombe et al., 1988*a*; Kao et al., 1989; Hernandez-Cruz et al., 1990; Niggli and Lederer, 1990), have been studied with the aid of these techniques.

Unfortunately, imaging techniques, traditionally based on the use of silicon intensified target (SIT) cameras, have not been implemented in skeletal muscle fibers since the fast Ca^{2+} transients in this preparation would be highly distorted by the slow and nonlinear response of the imager. These limitations are vastly reduced in charge coupled device (CCD) imagers which have the additional advantages of high resolution, low noise, wide dynamic range, and high photometric accuracy (Hiraoka et al., 1987). CCDs have been recently used, in conjunction with microchannel plate intensifiers, to obtain fast image recordings of indo-1 fluorescence transients in cardiac myocytes (Takamatsu and Wier, 1990), and in smooth muscle cells to acquire fura-2 images (Linderman et al., 1990).

Upon Ca^{2+} binding, the new fluorescent indicators fluo-3 and rhod-2 exhibit large increases in fluorescence without shifts in the excitation or emission spectra (Minta et al., 1989). Although this property precludes the use of ratiometric protocols, quantitative deconvolution of the fluorescence images can be achieved by alternative methods (Hesketh et al., 1983; Kao et al., 1989; DiFranco et al., 1990). At the peak absorption wavelengths of these dyes, conventional light microscopes can provide intensities of illumination significantly higher than at the ultraviolet (UV) region of the spectrum required by fura-2 and indo-1. This convenient illumination condition, accompanied by a high efficiency in fluorescence emission at wavelengths comfortably detected by CCD imagers, make these dyes optimal candidates for their use in the image detection of fast

0006-3495/91/01/12/13 $2.00

Ca^{2+} transients in skeletal muscle fibers. Moreover, these dyes have Ca^{2+} dissociation constants at least five-fold bigger than those reported for fura-2 and indo-1 (Grynkiewicz et al., 1985; Minta et al., 1989; Garcia et al., 1989). This makes them more suitable for the tracking of Ca^{2+} transients in skeletal muscle fibers, supposedly reaching levels in the micromolar range (Vergara and Delay, 1985; Hirota et al., 1989).

The purpose of the present article is to report on the use of the fluorescent Ca^{2+} indicators fluo-3 and rhod-2, and an inexpensive video system utilizing a commercial CCD camera, for the fast imaging detection of Ca^{2+} transients in skeletal muscle fibers. We present results validating the performance of this system by comparing video image data with analogue signals detected by a photodiode. We also report on technical additions to standard commercial equipment to configure a low cost imaging system which may be valuable for future practical applications. Finally, some observations on the Ca^{2+} release response to inositol (1, 4, 5)-trisphosphate ($InsP_3$) microinjected into single muscle fibers are presented to illustrate the space resolution of the imaging system and to demonstrate its usefulness in muscle research.

Some of the results presented here have been previously communicated in preliminary form (Garcia et al., 1989; DiFranco et al., 1990).

METHODS

Electrophysiological techniques

The general electrophysiological methodology was similar to that described elsewhere (Vergara et al., 1978; Heiny and Vergara, 1982; Palade and Vergara, 1982). Single skeletal muscle fibers were dissected from the semitendinosus muscle of the bullfrog *Rana catesbeiana* and mounted in a triple vaseline gap chamber (Hille and Campbell, 1976) situated on the stage of a compound microscope (Nikon Optiphot, Nikon Corp., Garden City, NY). The muscle fiber was extended across the vaseline partitions while immersed in an isotonic K_2SO_4 solution buffered at pH 7 with MOPS (3-[*N*-morpholino]propanesulfonic acid). The fiber was pinned down (at the end pools C and E, using minute stainless steel pins) to the bottom of the chamber lined with an elastomeric resin (Sylgard 182; Dow Corning Corp., Midland, MI); four pools were electrically isolated by lowering the level of the solution. The end pools' solutions were exchanged with an internal saline of the following composition: K-Aspartate, 110 mM; K-MOPS, 20 mM; K_2-ATP, 3 mM; Na_2-PCr, 5 mM; $MgCl_2$, 2 mM; creatine kinase, 0.1 mg/ml; EGTA, 10–50 μM; pH 7.0. The acid form of the fluorescent dyes rhod-2 or fluo-3 (Molecular Probes, Eugene, OR) was neutralized with K-OH and dissolved in the internal saline at concentrations ranging from 3 to 300 μM. The external saline in pool A, where the electrical and optical recordings were made, was continuously perfused with Ringer's solution. The temperature in this pool was measured with a thermistor and controlled by a feedback circuit driving two thermoelectronic heat exchanging units. The temperature could be rapidly adjusted to values ranging from 0 to 25°C, with an uncertainty of ± 1°C.

Two small incisions were made at each segment of the fiber in pools E and C, close to the vaseline seals, letting the contents of the internal solution equilibrate, by diffusion, inside the muscle fiber. The epifluorescence image of the segment of fiber in pool A was periodically monitored. In general, short times after the incisions were made, the dye was asymmetrically distributed due to intrinsic differences in the diffusion lengths from both ends. Homogeneous distribution of dye was usually attained after an equilibration period of 30 to 45 min; nevertheless, in some cases, uniform dye distribution was not reached.

Microiontophoresis

For the microinjection experiments, the muscle fibers were depolarized in an isotonic K_2SO_4 solution, which resulted in a phasic contracture, and then mounted in a relaxed state in the vaseline gap chamber. The ends were cut in internal solutions following the procedures described above; in this case, however, the isotonic K_2SO_4 added with 1 mM $CaCl_2$, was maintained as external perfusate in pool A. The micropipettes were pulled in a Brown-Flaming horizontal puller (Sutter Instruments Co., San Francisco, CA) from Kwik-fil glass capillaries (WPI, New Haven, CT) and had an average tip resistance of 10 Mohm when filled with 3 M KCl. They were mounted in a plastic holder and driven by a hydraulic micromanipulator (MO-103; Narishige, Tokyo). The shanks of the micropipettes were coated with Sylgard to reduce the distortion of the image field by the meniscus created at the entrance of the pipette to the external bath. The pipettes were oriented horizontally and approached the muscle fibers at a 90° angle. Just before the iontophoretic microinjections, freshly pulled pipettes were filled with small aliquotes (10 μl) of a solution containing 40 mM K-MOPS and 9 mM $InsP_3$. The interior of the micropipettes were connected through an Ag/AgCl wire electrode to the output of a current booster amplifier which received command pulses from the pulse generator under computer control. Iontophoretic current pulses were passed from the tip of the micropipette inside the muscle fiber, through the cut ends, to remote electrodes in pools E and C, minimizing the current flow across the surface membrane of the muscle fiber.

Optical setup

The microscope shown in Fig. 1 *A* was customized as follows: (*a*) the specimen stage was permanently fixed to the microscope's base, (*b*) the focusing mechanism was altered to allow for the movement of the optical head with respect to the stage, and (*c*) a custom-made hinge, connecting the optical head with the column, was added to the microscope to permit removal of the former from above the stage during the process of mounting the muscle fibers on the experimental chamber. Fig. 1 *B* shows a schematic diagram of the optical arrangement of the experimental setup. The microscope was equipped with a standard epifluorescence attachment. The light source for epifluorescence illumination was either a 100-W halogen lamp, or a 100-W high pressure mercury-arc lamp. Diascopic illumination was obtained by filtering the light from a 100-W tungsten-halogen lamp with interference filters, and focusing it (through the microscope's condenser) either directly onto the muscle fiber or onto the wide end of a tapered glass fiber optic placed underneath the muscle fiber. This type of illumination was used to capture direct images of the striation pattern at rest and during muscle contraction; in some control experiments, it was also used to compare the time course of diascopic fluorescence signals with movement artifacts monitored at a selected wavelength out of the excitation band of the fluorescent dye (see Fig. 3). Heat reflecting filters (#66.2450; Rolyn Optics, Covina, CA) were used in both illuminating conditions to minimize the background light reaching the detectors, and to reduce heating effects on the preparation.

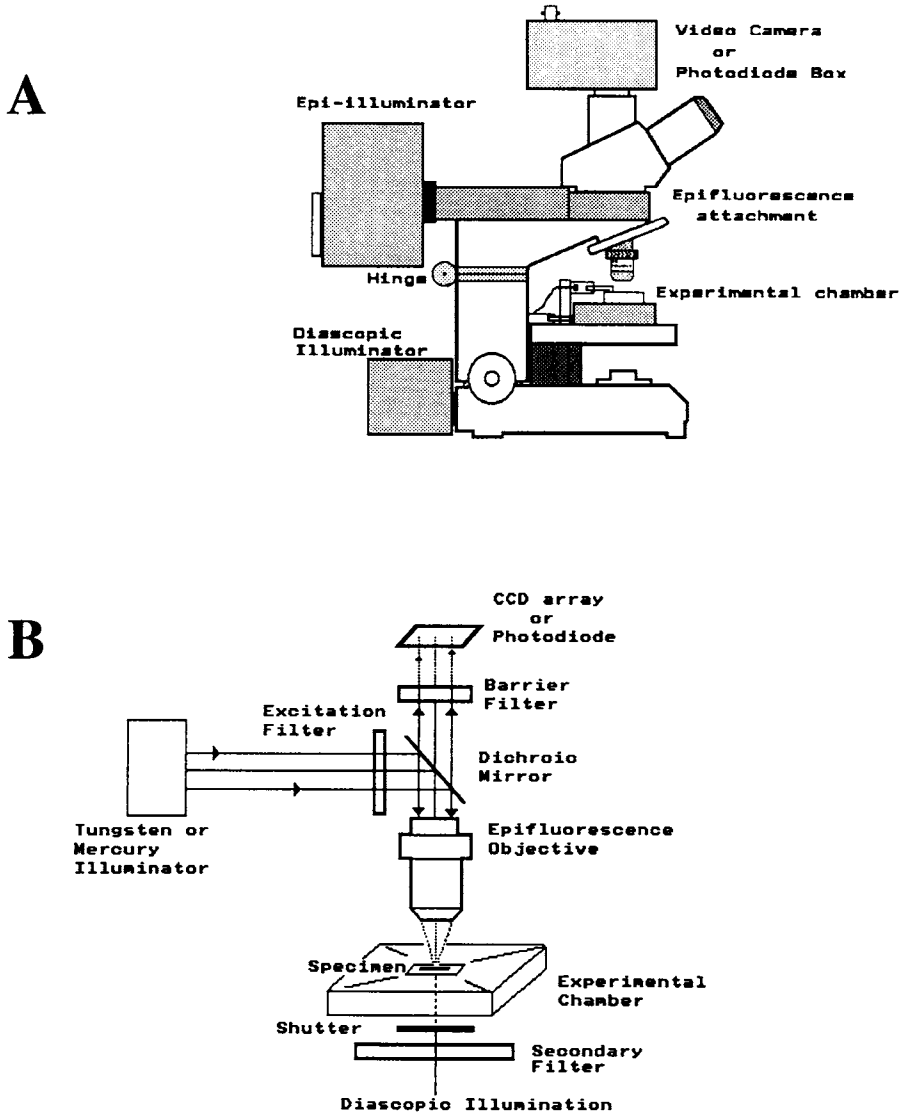

FIGURE 1 (*A*) Drawing of the microscope utilized in imaging experiments showing the precise location of the experimental chamber, optical detectors, illuminators, epifluorescence attachment, and the custom-made hinge. (*B*) Schematic diagram of the optical components and light paths within the microscope of Fig. 1 *A*. The excitation and barrier filters were mounted, together with the dichroic mirror, in a cube which was inserted in a slider carrier of the epifluorescence attachment. The cube could be moved in and out of the optical path to allow for episcopic and diascopic illumination, respectively. For diascopic fluorescence measurements (see Fig. 3), a barrier filter was inserted either in front of the detector (Fig. 3, trace *b*) or underneath the shutter (Fig. 3, trace *c*). For simultaneous diascopic and episcopic illumination (Fig. 4, panels *b* and *c*), the shutter was open leaving the cube in the light path.

Filter combinations tested to yield optimal fluorescence signals and video images with the dyes rhod-2 and fluo-3, using diascopic and episcopic illumination, are summarized in Table 1.

The image of the muscle fiber was directly formed, by a 20x fluorescence objective (Nikon Fluo20, N.A. 0.75), onto a light-sensitive device placed at the focal plane of the trinocular head port of the microscope. This device was either a photodiode (PV-100, EG&G Reticon Corp., Sunnyvale, CA), when continuous recordings of fluorescence Ca^{2+} transients were acquired, or the image detector of a CCD camera (described below), when fluorescence Ca^{2+} images were captured. Both devices could be readily interchanged while an experiment was underway, allowing for the acquisition of both types of optical records under each experimental condition.

The photodiode records were obtained using a current-to-voltage converter and track-and-hold circuit, similar to one described previously (Vergara et al., 1978), with a bandwidth from DC to 5 KHz. The optical signals were acquired together with the membrane action potentials by multiplexing them at the inputs of the data acquisition unit (see Fig 2). They were scaled dividing each trace by the baseline light intensity recorded immediately before stimulation. Optical data

TABLE 1 **Optimal filter configurations for the detection of fluorescence signals**

Fluorescent dye	Excitation filter C.W. ± H.W. or bandpass wavelengths	Dichroic mirror C.W.	Barrier filter cut-on or bandpass wavelengths
	nm	*nm*	*nm*
Diascopic illumination			
Fluo-3	480 ± 10	N/A	550*
Rhod-2	540 ± 10	N/A	570‡
Epifluorescence			
Fluo-3§	450–490	510	520–560
Rhod-2‖	510–560	580	590

Diascopic excitation filters were 2 × 2 inches (Ditric Optics Inc., Hudson, MA) and were placed below the preparation as shown in Fig. 1. Their optical properties are expressed as Center Wavelength (C.W.) ± Half Bandwidth (H.W.).
Epifluorescence excitation filters were 0.5 in circular plates that formed part of commercially available filter combinations. Their optical properties are given in terms of bandpass wavelengths.
*Schott glass filter OG-550.
‡Schott glass filter OG-570.
§Epifluorescence filter combination B-2E, Nikon. A less efficient combination tested was B-1A, Nikon (excitation/dichroic/barrier: 470-490/510/520).
‖Epifluorescence filter combination G-2A, Nikon (510-560/580/590). Another filter combination, made of 520-560/570/575 (Omega Optical, Inc., Brattleboro, VT) was almost equally efficient.

processed this way represented $\Delta I/I$ values for episcopic illumination (Fig. 3), or $\Delta F/F$ values for epifluorescence illumination (Fig. 5 *B*).

Image acquisition and display

A two-dimensional (572 × 485 pixels) CCD array of a commercial surveillance video camera (black and white, frame transfer, Sanyo VDC3800; Sanyo, Compton, CA) was used as the imaging device. This camera has a signal-to-noise (s/n) ratio better than 50 dB and does not generate after images. The composite video signal output of the camera complies with the EIA standard (525 lines, 60 fields/s, 1 Vpp). The camera was modified to disable the automatic gain control (AGC) internal circuitry to assure that the analogue video output was proportional to the light intensity over a wide range of luminance.

Fig. 2 shows a diagram of the electronic components used in the detection, acquisition and storage of video images, the acquisition and storage of electrical and optical transients, and the connections among

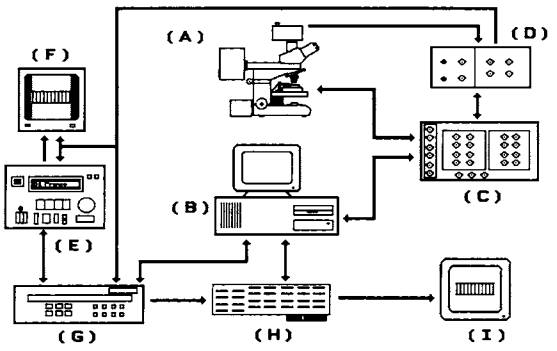

FIGURE 2 Simplified block diagram of the connections among the components of the imaging system. See text.

these components. This configuration provided proper synchronization between the fast electrical events occurring in the muscle fibers and the video imaging recording of the Ca^{2+} transients. The vertical synchronization pulses (V-sync) from the video camera (*A*) were used as a primary triggering signal that was distributed through a custom made synchronization unit (*D*) to the pulse generator and data acquisition unit (*C*; Axolab-1; Axon Instruments Inc., Foster City, CA) which operated under computer control (*B*; see below). The synchronization unit allowed to initiate a cycle of stimulation, acquisition, and video data recording, under program control, in synchrony with V-sync from the camera. This unit (*D*), in addition, mixed the video signal with a brief (10 μs) pulse displayed as a short horizontal line in the video image to indicate the instant at which the muscle fiber was electrically stimulated (see Fig. 5 *A*, *panel a*). The modified video signal was distributed to a monochrome monitor (*F*), an optical media data recorder (*G*; OMDR: TQ-2028F; Panasonic, Secaucus, NJ), a ¾″ video cassette recorder (*E*; VCR: U-Matic VO-5850, Sony Corp., Japan), and an 8-bit frame grabber with 640 × 512 pixel resolution (*H*; PC-1540, Chorus Data Systems, Merrimack, NH,). The latter device was inserted in an AT compatible computer (*B*; Data286-20; Dataworld, Inc., PicoRivera, CA) to provide on-line pseudocolor display at a digital high resolution monitor (*I*; Multiscan, CPD-1303; Sony Corp., Park Ridge, NJ). A special software package was written to program the sequential acquisition of images in the OMDR, synchronized with the electrical events during an experiment. Typically 15–30 sequential frames were stored in the OMDR per Ca^{2+} transient.

Analysis of video images

Images stored in the OMDR, or the VCR, were retrieved and acquired with the frame grabber for subsequent image processing and analysis. Commerical software (Imagepro, Media Cybernetics, Silver Spring, MD) and specially written software packages were used to signal average and linearize video images, to control of the OMDR for the sequential retrieval of images, and to delace fields from image frames. This latter procedure permitted to separate two 16.7-ms image fields from each standard interlaced video frame. Background compensation was performed by subtracting, to each image, the average of 10 frames

acquired while the camera port was closed. Because the autofluorescence of the fiber at the excitatory wavelengths for rhod-2 and fluo-3 was negligible, this average was equivalent to the image of the unstained fiber.

At moderate to high levels of luminance, the video camera behaved nonlinearly. Quantitative analysis of the images required the following linearization procedure: an intensity-transform table was constructed from the digital grey-levels (measured at the center of the image) acquired at varying intensities of illumination on the CCD. For this method, the intensity levels were obtained by filtering uniform monochromatic light with neutral density filters. The intensity-transform table gave the numeric factors used to multiply, pixel by pixel, the raw images to yield corrected images with a faithful intensity representation.

Image data is presented as follows: (*a*) Linearized fluorescence images are displayed in black and white, with 256 shades of gray mapping the levels of fluorescence intensity (Fig. 4, *d* and *e*), or in pseudocolor, with intensity levels mapped into colors according to palette bars (Fig. 6). (*b*) $\Delta F/F$ ratio images, generated from a pixel-by-pixel deconvolution of linearized images, using the expression: $\Delta F/F = (F - F_{rest}) / F_{rest}$, where F_{rest} are pixel values from the image of the fiber before electrical stimulation and F are the corresponding values from the 16.7-ms images acquired during a Ca^{2+} transient. The resulting images are displayed in a pseudocolor scale of $\Delta F/F$ values (Fig. 5 *A*).

The black and white and color pictures were photographed from the screen of the digital monitor (unit I in Fig. 3), using standard commercial films (respectively, Plus-X pan and Gold200; Eastman Kodak Co., Rochester, NY) and a photographic camera equipped with a macro lens. The black and white negatives were printed under conditions of controlled illumination to preserve the gray pattern observed on the monitor screen. The color pictures were custom printed by a commercial laboratory, taking care to preserve the color hues of the pseudocolor display.

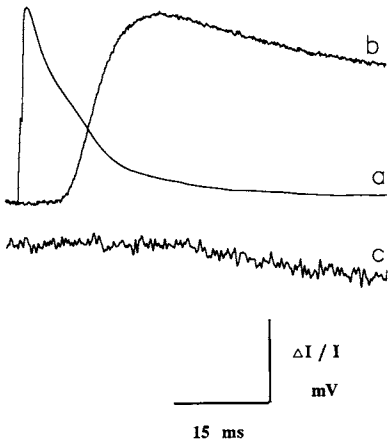

FIGURE 3 Temporal relations between action potential (trace *a*), rhod-2 diascopic fluorescence signal (trace *b*) and movement artifact (trace *c*). The source of illumination was a tungsten-halogen lamp and the movement artifact was obtained as described in the text. The ends of the muscle fiber were cut in an internal solution containing, in addition to the components described in Methods, 100 μM rhod-2 and 50 μM EGTA. The fiber was stretched to a sarcomere spacing of 2.6 and the resting membrane potential was held at −100 mV. The time axis is the same for all traces. The vertical bar represents 64 mV for trace *a*, 0.1 $\Delta I/I$ for trace *b*, and 0.02 $\Delta I/I$ for trace *c*. The fractional change in fluorescence ($\Delta F/F$) at the peak of the fluorescence signal (trace *b*) is 1.84. The temperature was set to 9°C.

RESULTS

Photodiode detection of rhod-2 calcium transients.

Fig. 3 demonstrates the temporal relationship between an action potential (*trace a*) and the early phase of the fluorescence signal (*trace b*) detected from a single muscle fiber stained intracellularly with 100 μM rhod-2. The fiber was illuminated diascopically with monochromatic light at a wavelength of 540 nm; the emitted light was filtered with a high pass barrier filter with a cut-on wavelength of 570 nm (Table 1). As a control, trace *c* shows the change in light intensity recorded when the barrier filter was placed between the muscle fiber and the excitation filter in the light path (see legend, Fig. 1 *B*). This manipulation eliminates the dye fluorescence contribution to the detector and provides evidence for changes in light scattering or absorption contributed by the mechanical activation of the muscle fiber. It can be seen that this movement artifact (*trace c*) differs from the rhod-2 fluorescence signal (*trace b*) in three aspects: (*a*) its magnitude, expressed in $\Delta I/I$ units, is significantly smaller (~ 25 times smaller) than the fluorescence peak; (*b*) it goes in the opposite direction: shows a reduction in transmitted light intensity as opposed to the fluorescence increase of the transient, which results from the binding of Ca^{2+} ions to the rhod-2 molecules; and (*c*) it shows a slower time course, being only perceptible after the peak was reached in the fluorescence signal.

Epifluorescence imaging

Fig. 4, panel *a*, shows the image, acquired with the video camera, of a quiescent muscle fiber stained with 8.5 μM rhod-2 and illuminated with high intensity monochromatic light. This image, that permits to appreciate the resolution of the imaging system, shows the typical striation pattern of the muscle fiber with a sarcomere spacing of ~ 3.6 μm. Images of this type were repeatedly acquired throughout the experiments to assess the overall appearance of the muscle fiber and to keep record of possible changes in fiber diameter. By lowering the intensity of the diascopic illumination and sliding in the epifluorescence cube (see Fig. 1 *B*), it was possible to obtain a mixed image in which the epifluorescence of the dye in the muscle fiber was comparable with the transmitted diascopic light through the fiber (Fig. 4, panels *b* and *c*). These pictures illustrate the projection of the epifluorescence cone of light on the muscle fiber. This type of

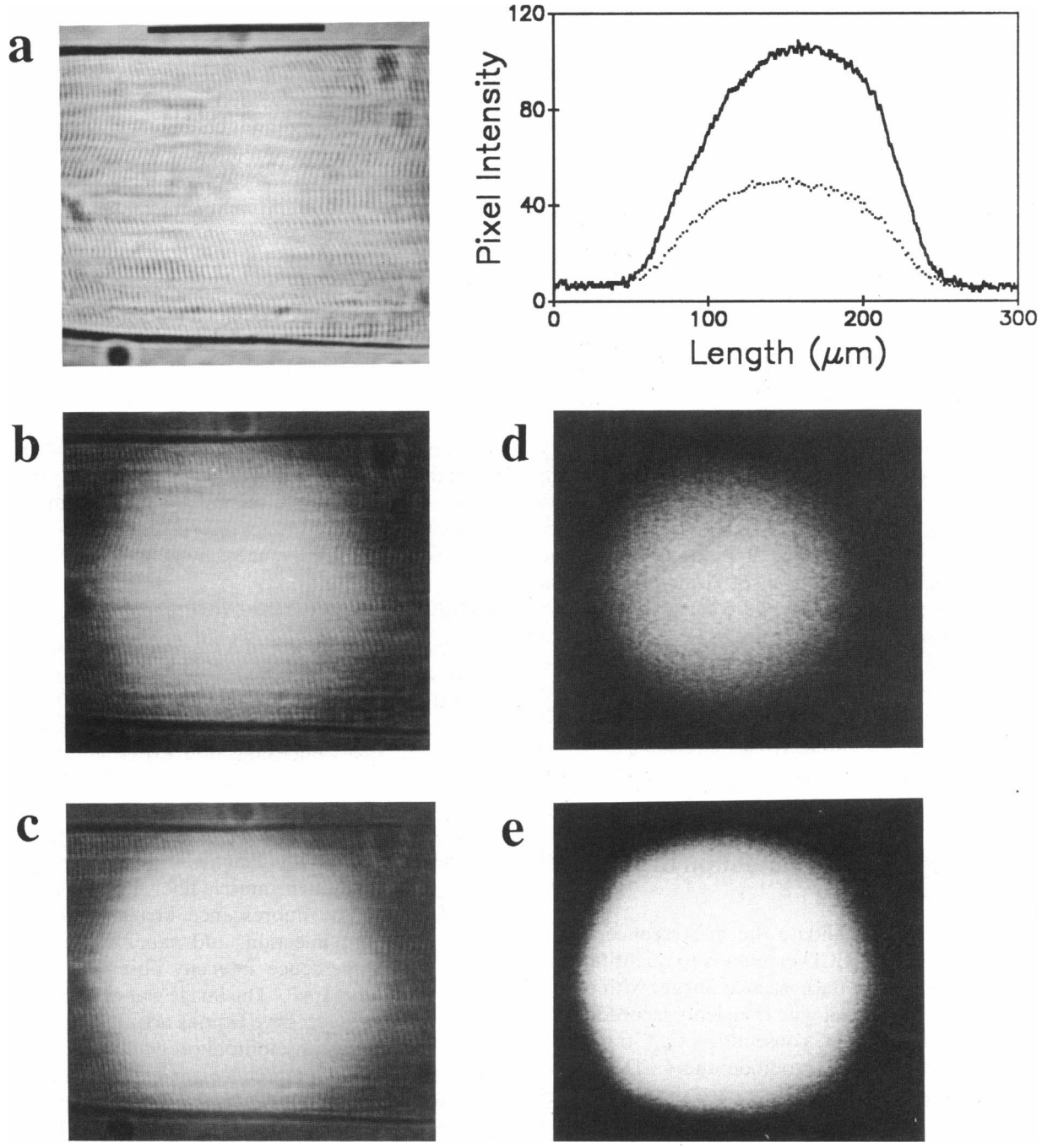

FIGURE 4 (*a*) Diascopic direct image of a segment of a single skeletal muscle fiber stained intracellularly with 8.5 μM rhod-2 and illuminated at a wavelength of 600 nm wavelength. The fiber was stretched to a mean sarcomere spacing of 3.6 μm. The calibration bar represents 100 μm. (*b*, *c*) Images of the same segment of fiber but simultaneously illuminated diascopically with light of lower intensity than in *a*, and episcopically at wavelengths selected with the cube G-2A (see Table 1). The source for episcopic illumination was a mercury-arc lamp. The diameter of the epifluorescence spot was adjusted to be similar to fiber diameter. The images are displayed at the standard black and white video output with a resolution of 256 gray levels. Each image corresponds to a single video frame; *b* is the image at rest and *c* is the image at the peak of the fluorescence transient. (*d*, *e*) The same as *b* and *c*, but displaying only the epifluorescence from which the background was subtracted. Temperature: 12°C. (*Inset*) Plot of the intensity profiles measured horizontally along the same axial row of pixels of the images in *d* and *e*. The dotted line corresponds to *d* and the continuous line to *e*. The maximal fractional change in fluorescence ($\Delta F/F$) computed from these profiles is 1.5.

imaging was useful and routinely used at the beginning of each experiment to center the cone of illumination on the muscle fiber, adjusting it to a diameter smaller than the length of pool A. Although this adjustment introduced the inconvenience that the shape of the fluorescent area had an apparent elliptical shape, rather than the rectangular profile of the muscle fiber (see also Fig. 5 *A*, below), it improves the resolution of the optical system and was necessary to avoid undesirable fluorescence contamination from the vaseline seals.

Epifluorescence images of the same fiber are displayed, in black and white, in Fig. 4, panels *d* and *e*. As seen, the standard 256 gray scale is not ideal to depict quantitative changes in intensity. In spite of that, the difference in fluorescence between the unstimulated image in panel *d*, comared with that acquired after electrical activation in panel *e*, is so remarkable that they were selected to illustrate what could be visualized with the naked eye. Panels *d* and *e* also show that the magnitude of the fluorescence enhancement experienced by the dye rhod-2 when it binds Ca^{2+}, is large enough to permit the detection of sizable changes in fluorescence even at very low dye concentrations. The inset in Fig. 4 shows a quantitative plot of the fluorescence along the fiber recorded before (*dotted line*) and after electrical stimulation (*continuous line*) as shown in panels *d* and *e*. It can be appreciated that the bell-shaped profile of the illuminated spot at rest is preserved for the higher intensities at the peak of the fluorescence change.

Image and photodiode detection of fluor-3 transients

A useful approach to validate the fluorescence image data obtained with the CCD camera is to quantitatively compare pixel values in fluorescence images with corresponding values along analogue transients recorded with a photodiode. To do that, consecutive Ca^{2+} transients were recorded with the photodiode and CCD camera, respectively. Fig. 5 *A* shows a sequence of $\Delta F/F$ images obtained as described in Methods from a fiber stained intracellularly with 195 μM fluo-3. The images used for these calculations were delaced from frames captured at the standard video rate of 30 frames/s. Panels *a–f* of Fig. 5 *A* display 6 out of 14 consecutive images during a Ca^{2+} transient, and illustrate the time course of the $\Delta F/F$ fluorescence changes. The horizontal white bar in panel *a* marks the instant at which the muscle fiber was stimulated with a 0.5-ms current pulse. The rise in $[Ca^{2+}]_i$ was evidenced by an increase $\Delta F/F$, which in this case is displayed as a change in the color pattern of the pseudocolor scale (varying from black to white; see pseudocolor scale inset, Fig. 5 *A*). The average $\Delta F/F$ of a small area (400 μm^2) at the center of each image field, increases from 0 (rest) to 4.6 at the peak (*panel b*). The continuous trace in Fig. 5 *B*, shows the time course of the Ca^{2+} transient recorded by the photodiode. This trace was obtained, without change, immediately before and after the image sequence of Fig. 5 *A*, thus verifying the reproducibility of the results. The average $\Delta F/F$ values at the center of each of 14 consecutive image fields (six of which are shown in Fig. 4 *A*) were scaled and superimposed on this trace to assess the fidelity of the image recording compared with the linear fast response of the photodiode. It can be observed that the images followed the time course of the transient detected by the photodiode with notable accuracy. As can be expected, the limited frequency response of the CCD camera produces a filtering effect on the images that spreads the time course of the reconstructed transient; nevertheless, this does not greatly distort the time course of the transient reconstructed from image data. This property emphasizes the usefulness of the CCD camera for quantitative measurements of light intensities.

Imaging of localized release of Ca^{2+}

An obvious application of a Ca^{2+} imaging system is the study of the mechanisms of Ca^{2+} release induced by topical delivery of agonists. To evaluate the performance of our optical system in that application, we performed $InsP_3$ microinjection experiments in single skeletal muscle fibers. Fig. 6, panel *a*, shows the area of impalement where a muscle fiber was iontophoretically microinjected with this agonist. The picture was retouched to outline the exact position of the tip of the micropipette inside the muscle fiber. Panel *b* displays, in pseudocolors, the fluorescence image of this precise area before the injection, and panel *d* illustrates the change in fluorescence intensity observed during the microinjection of $InsP_3$. The image was obtained from an average of five successive frames acquired 400 ms after the onset of a negative iontophoretic pulse. The perceptible change in fluorescence around the pipette tip, observed in response to the microiontophoresis of $InsP_3$, is better emphasized in Fig. 6, panel *c*, which was obtained by subtraction of panel *b* from panel *d*. It can be seen that images *b* and *d* only differ in the level of fluorescence of a circular area centered at the tip of the pipette. Control trials with positive current pulses were made before and after these images were acquired, and resulted in no obvious change in fluorescence.

DISCUSSION

This report describes a video imaging system which is especially suitable for the detection of fast epifluores-

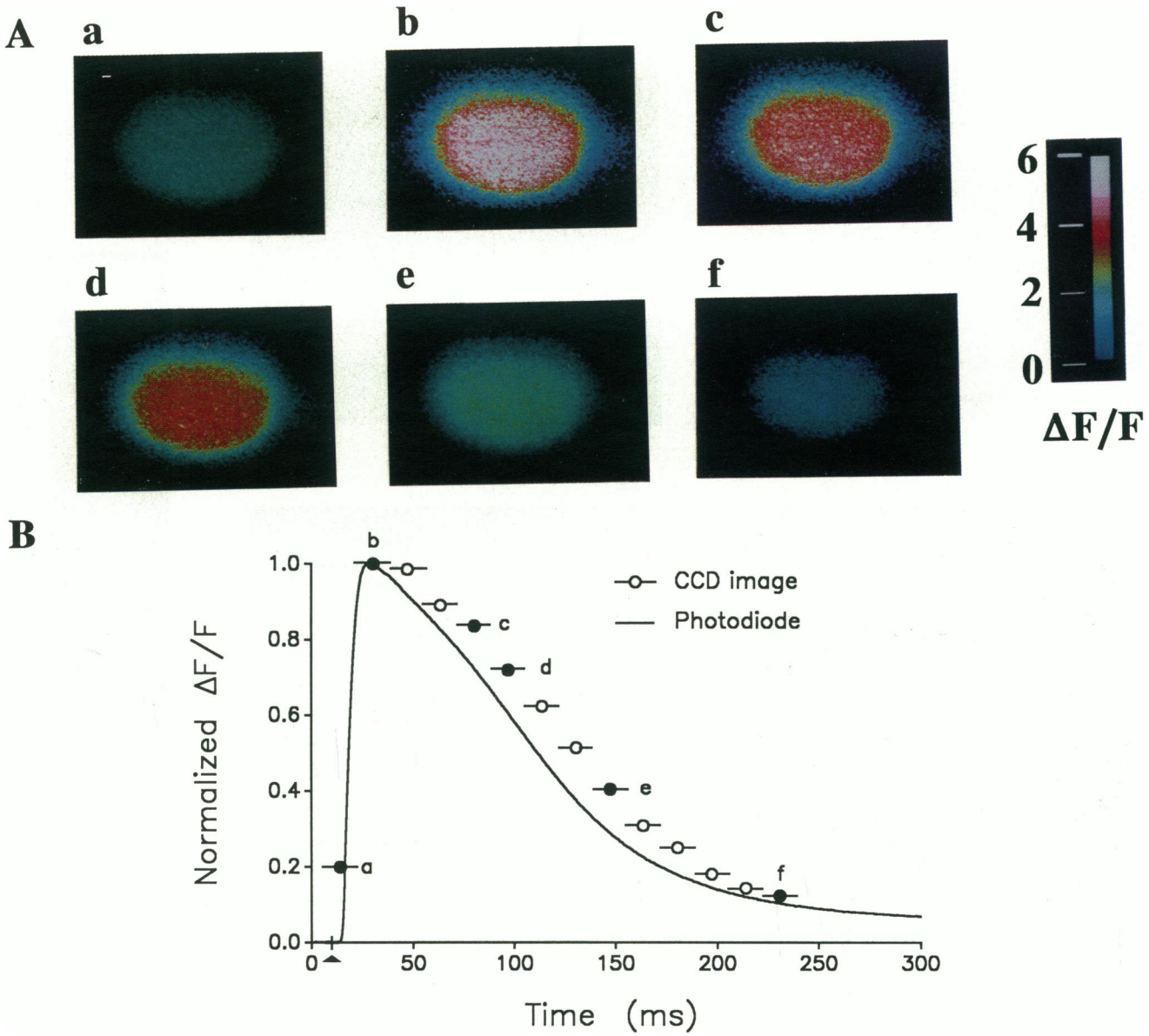

FIGURE 5 (*A*) $\Delta F/F$ images calculated from a series of 14 consecutive delaced video fields acquired during a Ca^{2+} transient elicited by action potential stimulation of a muscle fiber. The fiber was stained with 195 μM fluo-3 and episcopically illuminated with light coming from a tungsten-halogen lamp source. The sarcomeric spacing was 3.6 μm. The white line in the first video image (*a*) shows the exact time at which a 0.5-ms current pulse was delivered to the muscle fiber. The raw fluorescence images, used to calculate the $\Delta F/F$ images, were background compensated, and low-pass filtered (see Methods). The palette inset at the right illustrates pseudocolor scale matching a span of $\Delta F/F$ values from 0 to 6. The fiber diameter was 93 μm and the temperature was set to 8°C. (*B*) The continuous trace shows the fluorescence transient of the same fiber, but taken immediately before the image sequence of Fig. 5 *A*. The amplitude of the transient was normalized to a peak $\Delta F/F$ value of 3.5. The symbols (-○-) superimposed on the continuous trace correspond to average $\Delta F/F$ values measured in a square area of 400 μm^2 at the center of each of 14 successive images and normalized to a maximum of 4.6. The length of the symbols corresponds to the 16.7-ms integration time per field of the CCD camera. The black symbols (-●-), and the letters above them, indicate those images displayed in Fig. 5 *A*.

cence Ca^{2+} transients in skeletal muscle fibers. The methodology described here utilizes a commercial CCD camera which is available at a cost of a few hundred dollars, instead of the significantly more expensive SIT cameras required for fura-2 Ca^{2+} imaging. These techniques depend critically, and take advantage of, the properties of the fluorescent Ca^{2+} indicators fluo-3 and rhod-2, recently made available after the work of Tsien

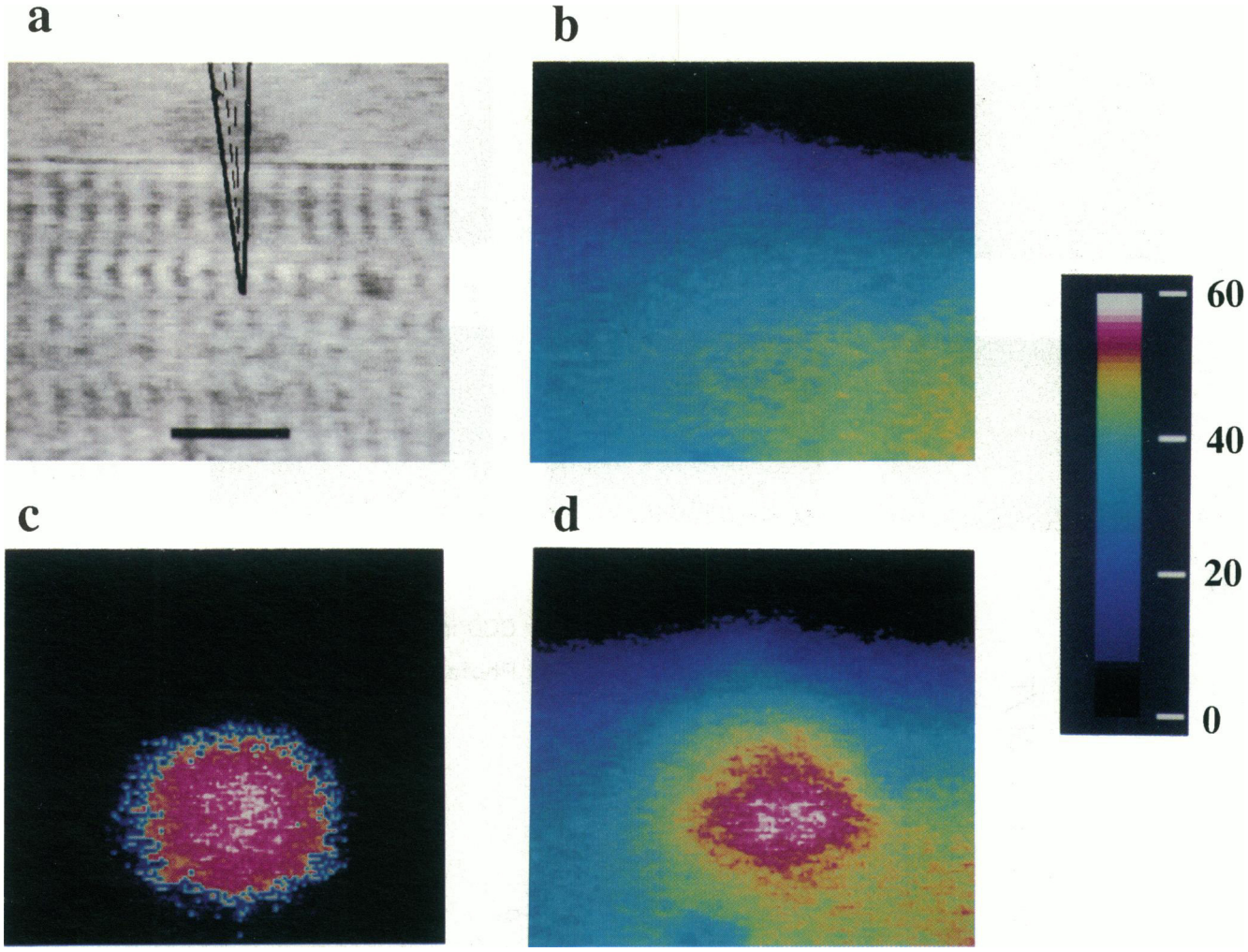

FIGURE 6 Changes in fluroescence induced by iontophoretical microinjection of $InsP_3$ into a muscle fiber. The fiber was diffused with ~200 μM rhod-2 and remained depolarized throughout the experiment in isotonic K_2SO_4. A 500-ms pulse was used to deliver the drug through a pipette with a tip resistance of 10 Mohm. *a* shows the site of the micropipette impalement of the muscle fiber as observed with diascopic illumination. The calibration bar corresponds to 10 μm. *b* shows the epifluorescence image before the injection. *d* corresponds to images acquired ~400 ms after the beginning of the iontophoretic pulse. *c* was obtained by subtraction of image *b* from image *d* and then multiplied by a factor of three. Each image was an average of five successive video frames. Images *b* to *d* were background subtracted and low pass filtered. The pseudocolor palette at the right of the figure shows the color correspondence within the pixel intensity range 0–60.

and collaborators (Minta et al., 1989; Kao et al., 1989). These dyes undergo large fluorescence changes upon Ca^{2+} binding, absorbing excitatory light and fluorescing in the visible range of the light spectrum. The peak emission wavelengths of these dyes, 510 and 570 nm for fluo-3 and rhod-2, respectively, are readily detected by the pixel elements of CCD cameras, avoiding the use of image intensification components which are expensive and may have undesirable properties for the detection of fast events.

Very recently, Takamatsu and Wier (1990) described a ratiometric imaging system, based on the use of indo-1, which is capable to acquire up to four consecutive images with a time resolution comparable to our system. They used it to image Ca^{2+} concentration changes in voltage-clamped single cardiac myocytes that occur with a slower kinetics than those in skeletal muscle fibers.

In this paper we present, for the first time, consecutive fluorescence images, acquired every 16.7 ms, during a Ca^{2+} transient elicited by electrical stimulation of a single skeletal muscle fiber. In this experiment, photodiode and image data are expressed in $\Delta F/F$ units according to the definition: $\Delta F/F = (F - F_{rest})/F_{rest}$, described previously (Vergara et al., 1978; Cornell-Bell

et al., 1990). This procedure allows for a quantitative comparison of pixel intensities in image data with corresponding analogue levels of the photodiode signals. We did not calibrate the magnitude of the fluorescence intensity changes in terms of myoplasmic-free $[Ca^{2+}]_i$ concentrations because those determinations require the inclusion of a number of control images and calibration procedures that will be presented in future publications from our laboratory and go beyond the scope of this paper.

Photodiode detection of fluo-3 and rhod-2 Ca^{2+} transients

As previously reported (Garcia et al., 1989; DiFranco et al., 1990), the fluorescence signals detected by photodiode from electrically stimulated skeletal muscle fibers stained with rhod-2 or fluo-3 (Figs. 3 and 5 *B*), show a time course comparable to those previously reported with other Ca^{2+} indicators (Baylor et al., 1982; Miledi et al., 1982; Palade and Vergara, 1982; Kovacz et al., 1983; Vergara and Delay, 1986). An important characteristic of these records is their excellent s/n ratio which is mainly due to the optimal quantum efficiency and spectral properties of these fluorescent dyes (Tsien, 1988; Minta et al., 1989; Kao et al., 1989). Changes in fluorescence are large compared with the background noise of the photodiode, therefore generating virtually noiseless epifluorescence signals (see Figs. 3 and 5 *B*). Using high pressure mercury arc illuminators, we have been able to detect Ca^{2+} transients with very large s/n ratio from fibers stained intracellularly with end pool concentrations of rhod-2 as low as 3 μM (DiFranco and Vergara, unpublished results). Results similar to those shown in Fig. 3 suggest that fluo-3 and rhod-2 permit to detect uncontaminated Ca^{2+} fluorescence signals due to the low interference from movement artifacts in stretched, but contracting, fibers (sarcomere spacings between 2.6 and 3.6 μm). The movement artifacts become more prominent in unstretched fibers, but rarely reached levels amounting to more than 10% of the fluorescence signals, making these techniques ideal for the detection of transients in fully contracting muscle fibers.

Image detection of Ca^{2+} transients

Photodiodes have been traditionally used in the detection of optical signals generated by Ca^{2+} indicating dyes because of their high quantum efficiency, low noise, fast frequency response, excellent linearity, and reasonable sensitivity. These devices integrate the discrete intensity contributions arising from different points of a specimen whose image is formed on the photosensitive area and, consequently, do not provide topological information about structural features of the specimen. In contrast, CCDs and other imager devices, display a two-dimensional portrait of the intensities of an image formed on an array of active elements.

An important technical feature of the imaging system described here is the capability to acquire and store, in real time, up to 16,000 consecutive fluorescence images in synchrony with electrophysiological stimuli. This property is attained by the design of the synchronization unit (*D* in Fig. 2) in conjunction with a commercial OMDR (*G* in Fig. 2) and a specially written software package to control the overall imaging system.

With this system, we have been able to prove that CCD cameras can be used for the detection of events as fast as the Ca^{2+} transient in a skeletal muscle fiber with a frequency response limitation intrinsic to the rastering of the CCD array (16.7 ms). This is convincingly demonstrated by the similarity between the continuous time course of the Ca^{2+} transient detected with a photodiode and the temporal reconstruction of scaled $\Delta F/F$ images shown in Fig. 5 *B*. CCD images track reasonably well the overall time course of Ca^{2+} transients at moderately low temperatures like those used in these experiments (8–12°C). Unfortunately, the imaging system is able to acquire only one image during the rising phase of the fluorescence transients at these temperatures. At lower temperatures, the situation improves, but at higher temperatures, the infrequent sampling by the imaging system should significantly distort the image representation of the fluorescence transient because its peak level is reached at shorter times and the overall process is speeded up. This limitation has been overcome recently by a modification of the internal circuitry of the Sanyo VDC3800 camera, designed to scan restricted areas of the CCD array during fractions of the standard integration period of 16.7 ms (Roos and Parker, 1990; Vergara, J., J. Parker, M. DiFranco, I. Murciano, and K. Roos, unpublished results). This modification has recently allowed us to acquire consecutive fluorescence images every 4 ms during a Ca^{2+} transient in single skeletal muscle fibers (DiFranco and Vergara, 1990).

The images presented in Fig. 5 *A* show an elliptical shape limited by the borders of the muscle fiber and by the boundary of the illumination spot (see also Fig. 4). Although these images reflect closely the changes in $[Ca^{2+}]_i$ inside the muscle fiber, they have not been processed to yield the true value of $[Ca^{2+}]_i$. Although fluo-3 and rhod-2 are not ratiometric dyes, the quantitative deconvolution of the fluorescence images into $[Ca^{2+}]_i$ can be achieved by in vivo calibration methods which give highly reproducible results (Hesketh et al., 1983; Kao et al., 1989). We employed a modified method, based on the use of a Ca^{2+}-saturation image acquired at

the end of each experiment, to deconvolute fluorescence intensity images (such as those shown here) into $[Ca^{2+}]_i$ images (DiFranco et al., 1990). Some important features of these $[Ca^{2+}]_i$ images are the absence of the elliptical pattern given by the geometry of the illuminating spot, and the reasonable values calculated for the peak myoplasmic $[Ca^{2+}]_i$ during a transient (DiFranco et al., 1990; DiFranco and Vergara, 1990).

We calculate that our optical system has a limit of resolution of ~0.4 μm (Inoue, 1986) and a depth of field of 1.5 μm (Sheppard, 1987). Although digital image processing permits to recover undergraded images from raw images containing contributions from out-of-focus sections of a thick specimen like the muscle fiber, an exhaustive knowledge of the optical system point spread function (PSF) or its Fourier transform, the optical transfer function (OTF) will be required (Castleman, 1979; Hiraoka et al., 1987, 1990). A simple method for the experimental determination of the OTF of an epifluorescence imaging system like ours has been recently described (Hiraoka et al., 1990). This methodology is encouraging for future studies, but poses several complexities that need to be tested in relation to Ca^{2+} imaging techniques; at this early stage of development of our optical system, we limited ourselves to present images with minimal processing. Nevertheless, we believe that optical sectioning analysis of fluorescence images like those shown here, represents an excellent alternative to confocal microscopy, another methodology designed to minimize the problem of out-of-focus information in fluorescence microscopy (White et al., 1987; Hernandez-Cruz et al., 1990; Niggli and Lederer, 1990).

Advantages of imaging detection methods for muscle research

An obvious advantage of the imaging methodology described in this paper is the convenience of following the physiological structural changes occurring during mechanical activation and concomitantly record fluorescence intensity changes associated with variations in $[Ca^{2+}]_i$. For example, in relation to the sequence of fluorescence images shown in Figs. 4 and 5, we observed that the onset of mechanical activation, defined as the time at which the earliest movement of sarcomeres could be detected, lagged behind the onset of the fluorescence transient by about one or two image fields. The two time courses diverged in time, leading to a separation between the peak of the Ca^{2+} transient and the peak of the mechanical response of about six frames at 10°C; these figures changed slightly, depending on the experimental conditions. The dynamic relationship between Ca^{2+} and movement images during isometric contractions emphasizes the applicability of the methodology illustrated here to study interesting aspects of muscle physiology.

Another major advantage of the Ca^{2+} image detection system described here is that, in addition to the ability to follow fast events, it still maintains the quality of imager devices to track very slowly changing phenomena which may be heterogeneously distributed within the bulk of the muscle fiber. This function, which cannot be performed by a photodiode system, will be of great help in the future of muscle research for the determination of the steady state $[Ca^{2+}]_i$ at conditions that modify the fast Ca^{2+} release in response to electrical stimulation.

An important advantage of fluo-3 and rhod-2 over fura-2 and quin-2 is that their spectral characteristics make it possible to use them as Ca^{2+} indicators simultaneously with UV flash photolysis of *caged* compounds (Minta et al., 1989; Kao et al., 1989; Tsien, 1988). Our results further demonstrate that it will be feasible to track the resulting changes in $[Ca^{2+}]_i$, in response to photorelease of chemical agents, not only with a photodiode but with a CCD camera generating a fast sequence of fluorescence images.

Microinjection experiments

Our system has enabled us to report, for the first time, video images demonstrating the $InsP_3$-induced release of Ca^{2+} during microinjection of the drug into depolarized muscle fibers. Although this will be an area of interesting applicability for imaging techniques in the study of muscle physiology, this data was shown with the purpose of illustrating our ability to picture localized time-dependent events in which Ca^{2+} ions participate. The processes underlying this simple observation may be very complex to analyze and are out of the scope of this publication. Suffice it to say that the circle of high fluorescence around the microinjection pipette probably reflects a spherical diffusion process which somehow involved the release of $[Ca^{2+}]$ in response to a local increase in the $InsP_3$ concentration. The first perceptible change in fluorescence was detected at the tip of the pipette ~360 ms before the fluorescence intensity spot grew to its maximal diameter of ~20 μm. Clearly this process occurred within the millisecond time domain, as suggested from the video analysis of mechanical responses to $InsP_3$ injections (Vergara et al., 1987) and contrary to the proposal that the response to $InsP_3$ may take seconds in skeletal muscle fibers (Walker et al., 1987).

Experiments on the detection of Ca^{2+} transients in skeletal muscle fibers with the dyes rhod-2 and fluo-3 were performed, previously to those reported here, in collaboration with Drs. J. Garcia and E. Stefani. We gratefully acknowledge their contribution. We are deeply

indebted to Mr. John Parker and Mr. Isaac Murciano for their technical support on the adaptation of the video camera for the purpose of fluorescence detection, and in the design of different elements of the video imaging setup. We thank them and Dr. K. Roos for helpful comments regarding the specific use of the Sanyo video camera in the present experiments. We are also thankful to Dr. M. Sanderson for his help in the development of a video software package and for helpful comments.

This work was supported by the National Institute of Health (NIH) grant AR-25201 and by the Muscular Dystrophy Association. Dr. DiFranco was partially supported by a fellowship from CONICIT, Venezuela. Dr. Suarez-Isla was partially supported by CONICYT, Chile and NIH grant GM 35981.

Received for publication 7 February 1990 and in final form 29 August 1990.

REFERENCES

Baylor, S. M., W. K. Chandler, and M. W. Marshall. 1982. Use of metallochromic dyes to measure changes in myoplasmic calcium during activity in frog skeletal muscle fibres. *J. Physiol.* 331:39–177.

Baylor, S. M., and S. Hollingworth. 1988. Fura-2 calcium transients in frog skeletal muscle fibres. *J. Physiol.* 403:151–192.

Blinks, J. R., R. Rudel, and S. R. Taylor. 1978. Calcium transients in isolated amphibian muscle fibers: detection with aequorin. *J. Physiol.* 277:291–323.

Cannell, M. B., J. R. Berlin, and W. J. Lederer. 1987. Intracellular calcium in cardiac myocytes: calcium transients measured using fluorescence imaging. *In* Cell Calcium and the Control of Membrane Transport. L. J. Mandel and D. C. Eaton, editors. Rockefeller University Press, NY. 202–214.

Castleman, K. R. 1979. Digital Image Processing. Prentice-Hall, Inc., NJ. 347–360.

Cornell-Bell, A. H., S. M. Finkbeiner, M. S. Cooper, and S. J. Smith. 1990. Glutamate induced calcium waves in cultured astrocytes: long-range glial signaling. *Science (Wash. DC).* 247:470–473.

DiFranco, M., D. Compagnon, and J. Vergara. 1990. Image analysis of calcium transients in skeletal muscle fibers. *Biophys. J.* 57:168*a*. (Abstr)

DiFranco, M., and J. Vergara. 1990. Ultrafast imaging of calcium transients in skeletal muscle fibers. *Acta Cientifica Venezolana.* In press.

Garcia, J., D. Compagnon, J. Vergara, and E. Stefani. 1989. Myoplasmic Ca^{2+} transients measured with rhod-2 and fluo-3 in single skeletal fibers from rat and frog. *Biophys. J.* 55:307*a*. (Abstr.)

Grynkiewicz, G., M. Poenie, and R. Y. Tsien. 1985. A new generation of Ca^{2+} indicators with greatly improved fluorescence properties. *J. Biol. Chem.* 260:3440–3450.

Hernandez-Cruz, A., F. Sala, and P. R. Adams. 1990. Subcellular calcium transients visualized by confocal microscopy in a voltage-clamped vertebrate neuron. *Science.* 247:858–862.

Heiny, J., and J. Vergara. 1982. Optical signals from the surface and T-system membranes in skeletal muscle fibers. *J. Gen. Physiol.* 80:203–230.

Hesketh, T. R., G. A. Smith, J. P. Moore, M. V. Taylor, and J. C. Metcalfe. 1983. Free cytoplasmic calcium concentration and the mitogenic stimulation of lymphocytes. *J. Biol. Chem.* 258:4876–4882.

Hirota, A., W. K. Chandler, P. L. Southwick, and A. S. Waggoner. 1989. Calcium signals recorded from two new purpurate indicators inside frog cut twitch fibers. *J. Gen. Physiol.* 94:597–631.

Hille, B., and D. T. Campbell. 1976. An improved vaseline-gap voltage-clamp for skeletal muscle fibers. *J. Gen. Physiol.* 67:265–293.

Hiraoka, Y., W. J. Sedat, and D. A. Agard. 1987. The use of a charge-coupled device for quantitative optical microscopy of biological structures. *Science (Wash. DC).* 238:36–41.

Hiraoka, Y., W. J. Sedat, and D. A. Agard. 1990. Determination of three-dimensional imaging properties of a light microscope system. Partial confocal behavior in epifluorescence microscopy. *Biophys. J.* 57:325–333.

Inoue, S. 1986. Video Microscopy. Plenum Press, New York. 118.

Kao, J. P. Y., A. T. Harootunian, and R. Y. Tsien. 1989. Photochemically generated cytosolic calcium pulses and their detection by fluo-3. *J. Biol. Chem.* 264:8179–8184.

Kawanishi, T., L. M. Blank, A. T. Harootunian, M. T. Smith, and R. Y. Tsien. 1989. Ca^{2+} oscillations induced by hormonal stimulation of individual fura-2-loaded hepatocytes. *J. Biol. Chem.* 264:12859–12866.

Kovacz, L., E. Rios, and M. F. Schneider. 1983. Measurements and modification of free calcium transients in frog skeletal muscle fibers by a metallochromic indicator dye. *J. Physiol.* 343:161–196.

Linderman, J. J., L. J. Harris, L. L. Slakey, and D. J. Gross. 1990. Charge-coupled device imaging of rapid calcium transients in cultured arterial smooth muscle cells. *Cell Calcium.* 11:131–144.

Lipscombe, D., D. V. Madison, M. Poenie, H. Reuter, R. W. Tsien, and R. Y. Tsien. 1988*a*. Imaging of cytosolic Ca^{2+} transients arising from Ca^{2+} stores and Ca^{2+} channels in sympathetic neurons. *Neuron.* 1:355–365.

Lipscombe, D., D. V. Madison, M. Poenie, H. Reuter, R. W. Tsien, and R.Y. Tsien. 1988*b*. Spatial distribution of calcium channels and cytosolic calcium transients in growth cones and cell bodies of sympathetic neurons. *Proc. Natl. Acad. Sci. USA.* 85:2398–2402.

Miledi, R., I. Parker, and G. Schalow. 1977. Measurement of calcium transients in frog muscle by the use of arsenazoIII. *Proc. R. Soc. Lond. B.* 198:201–210.

Miledi, R., I. Parker, and P. H. Zhu. 1982. Calcium transients evoked by action potentials in frog twitch muscle fibers. *J. Physiol.* 333:655–679.

Minta, A., J. P. Y. Kao, and R. Y. Tsien. 1989. Fluorescent indicators for cytosolic calcium based on rhodamine and fluorescein chromophores. *J. Biol. Chem.* 264:8171–8178.

Niggli, E., and W. J. Lederer. 1990. Real-time confocal microscopy and calcium measurements in heart muscle cells: towards the development of a fluorescence microscope with high temporal and spacia resolution. *Cell Calcium.* 11:121–130.

Palade, P., and J. Vergara. 1982. ArsenazoIII and antipyrylazoIII calcium transients in single skeletal muscle fibers. *J. Gen. Physiol.* 79:679–707.

Roos, K. P., and J. M. Parker. 1990. A low cost two-dimensional digital image acquisition sub-system for high speed microscopic motion detection. *Proc. Soc. Photo-Optical Inst. Eng.* In press.

Sheppard, C. J. R. 1987. Depth of field in optical microscopy. *J. Microsc.* 149:73–75.

Takamatsu, T., and W. G. Weir. 1990. High temporal resolution video imaging of intracellular calcium. *Cell Calcium.* 11:111–120.

Tsien, R. Y. 1988. Fluorescence measurement and photochemical manipulation of cytosolic free calcium. *Trends Neurosci.* 11:419–424.

Vergara, J., F. Bezanilla, and B. M. Salzberg. 1978. Nile blue fluorescence signals from cut single muscle fibers under voltage or current clamp conditions. *J. Gen. Physiol.* 72:775–800.

Vergara, J., and M. Delay. 1985. The use of metallochromic Ca indicators in skeletal muscle. *Cell Calcium.* 6:119–132.

Vergara, J., and M. Delay. 1986. A transmission delay and the effect of temperature at the triadic junction of skeletal muscle. *Proc. R. Soc. Lond. B.* 229:97–110.

Vergara, J., K. Asotra, and M. Delay. 1987. A chemical link in excitation-contraction coupling in skeletal muscle. *In* Cell Calcium and the Control of Membrane Transport. L. J. Mandel and D. C. Eaton, editors. Rockefeller University Press, New York. 133–151.

Walker, J. W., A. B. Somlyo, Y. E. Goldman, A. P. Somlyo, and D. R. Trentham. 1987. Kinetics of smooth and skeletal muscle activation by laser photolysis of caged inositol 1,4,5-trisphosphate. *Nature* (*Lond.*). 325:249–252.

White, J. G., W. B. Amos, and M. Fordham. 1987. An evaluation of confocal versus conventional imaging of biological structures by fluorescence light microscopy. *J. Cell Biol.* 105:41–48.

Wier, W. G., M. B. Cannel, J. R. Berlin, E. Marban, and W. J. Lederer. 1987. Cellular and subcellular heterogeneity of $[Ca^{2+}]_i$ in single heart cells revealed by Fura-2. *Science* (*Wash. DC*). 235:325–328.

Williams, D. A., K. E. Fogarty, R. Y. Tsien, and F. S. Fay. 1985. Calcium gradients in single smooth muscle cells revealed by the digital imaging microscopy using fura-2. *Nature* (*Lond.*). 318:558–561.